SKYSHINE CALCULATIONS FOR A LARGE SPENT NUCLEAR FUEL STORAGE FACILITY WITH SCALE 6.2.3*

GEORGETA RADULESCU,† KAUSHIK BANERJEE, THOMAS M. MILLER,
and DOUGLAS E. PEPLOW

Nuclear Energy and Fuel Cycle Division
Oak Ridge National Laboratory, Oak Ridge, Tennessee, USA

†P.O. Box 2008, Bldg. 5700

Oak Ridge, TN 37831-6170 USA

Telephone: (865) 241-9998

Fax: (865) 576-3513

E-mail: radulescug@ornl.gov

For submission to
Nuclear Technology

Total number of pages: 40
Total number of figures: 13
Total number of tables: 1

† To whom correspondence should be addressed.

ABSTRACT

The SCALE code system developed at Oak Ridge National Laboratory includes state-of-the-art capabilities for radiation source term and radiation transport simulations that can be used in numerous applications, including dose rate analyses of complex consolidated interim storage facilities (CISF). A licensed CISF could be used to store tens of thousands of metric tons of spent nuclear fuel discharged from commercial power reactors using various cask and storage pad designs. A CISF design must comply with the regulatory requirements provided in 10 CFR Part 72, including requirements related to annual dose limits applicable to real individuals located beyond the area controlled by the licensee. Therefore, calculating a dose to the public is a necessary part of the licensing process for the construction of a CISF. These calculations are very challenging because of the complexity of the CISF design and the low magnitude of dose rate at large distances from the facility. This paper describes detailed far-field dose rate calculations performed for a proposed CISF using MAVRIC, the Monte Carlo radiation shielding sequence in SCALE 6.2.3 with automated variance reduction based on discrete ordinates calculations. The method presented in this paper uses a detailed Monte Carlo radiation transport simulation in one step from source to dose rate. A series of independent simulations was made using the complete site geometry (all casks present) but with only one cask containing radiation sources to obtain the dose rate maps produced by each storage cask. The CISF dose rate map was obtained by adding the dose rate maps produced by the independent individual cask simulations. Ample volumes of air and soil extending beyond the location of interest for dose rate calculation were included in the calculation model to properly simulate important radiation attenuation and scattering events that affect far-field dose rates. A comprehensive sensitivity study is included in this paper to illustrate the

importance of selecting appropriate air volume, mass density, and composition for CISF skyshine dose rate calculations. Dry soil and soil containing water were analyzed to determine their effects on groundshine radiation.

Keywords: shielding, skyshine, consolidated interim storage facility

I. INTRODUCTION

Consolidated interim storage facilities (CISFs) are components of the US Department of Energy's current integrated waste management strategy. The purpose of a CISF would be to store a large fraction of the spent nuclear fuel (SNF) and associated waste such as Greater Than Class C (GTCC) low-level radioactive waste (LLRW) discharged from commercial power reactors. GTCC LLWR has radionuclide concentrations exceeding the Class C LLRW as defined in 10 CFR 61.55[1] and requires isolation from the human environment for a long period of time. The SNF currently stored at various reactor sites, both shutdown and operating, would be relocated to a CISF. A CISF must comply with the regulatory requirements in 10 CFR Part 72.[2] The 10 CFR 72 provides requirements, procedures, and criteria for the issuance of licenses to receive, transfer, and possess power reactor spent fuel, power reactor–related GTCC waste, and other radioactive materials associated with spent fuel storage in an independent spent fuel storage installation (ISFSI). Dose rate limits for any individual who is located beyond the controlled area of the storage facility are established in 10 CFR 72.104. During normal operations and anticipated occurrences, the annual dose equivalent to any individual who is located beyond the controlled area must not exceed 0.25 mSv (25 mrem) to the whole body, 0.75 mSv (75 mrem) to the thyroid, and 0.25 mSv (25 mrem) to any other critical organ. Therefore, the physical boundary of a CISF facility must be determined based on all sources of radiation at the CISF, including direct radiation and any released radioactive materials in effluents.

Calculating a dose to the public is a necessary part of the licensing process for the construction of a CISF. These calculations are very challenging because of the complexity of the CISF design and the low magnitude of the dose rate at large distances from the facility, which is much lower than that of the background radiation. For example, the dose rate corresponding to the average

background radiation exposure in the US is approximately 4.1×10^{-4} mSv/h.[3] Therefore, detailed simulation of radiation transport for a large CISF would require significant computing resources because of the complexity of the models that would describe many hundreds of storage casks, as well as ample volumes of air and soil beyond the storage pads. A two-step method that requires modest computing resources is often used in license applications. The purpose of the first step of this method is to determine energy and angular distributions on the cask external surface of the neutrons and photons exiting a storage cask. The surface source is then used in a new radiation transport calculation to determine dose rate as a function of distance from the storage facility. One drawback of this approach is that the space/energy/angle distribution of the particles coming off the cask needs to be binned, stored, and then resampled in the second step. The method presented in this paper uses a detailed Monte Carlo radiation transport simulation in one step (from source to dose rate), which is expected to yield more accurate results and be simpler to set up and run than the two-step method. MAVRIC,[4] the Monte Carlo radiation transport sequence in the SCALE 6.2.3 code system[5] developed at Oak Ridge National Laboratory (ORNL), is used in these calculations. SCALE 6.2.3 capabilities for radiation source and radiation transport simulations are described in Section II.

The dose rate at a location external to a storage cask is produced by photon and neutron radiation escaping from the cask and reaching that location unobstructed or through multiple scattering interactions with nuclei/atoms in the environment (e.g., air, soil, concrete). The contribution of the scattered radiation to the total dose rate increases with increasing distance from the storage cask.[6] Ample volumes of air and soil extending beyond the location of interest for dose rate calculation are typically included in the calculation model to properly simulate important radiation scattering events that contribute to the dose rate at that location. Air density, which varies

as a function of altitude and weather conditions, is a very important input parameter in these skyshine calculations. Because air density decreases with increasing altitude, less air attenuation occurs at high altitude compared to sea level. Water content in moist air decreases the rate of photon attenuation and increases neutron slowing down and absorption relative to dry air. Soil composition, especially its water content, also has significant effects on its neutron attenuation properties. Therefore, simulation of local atmospheric and environment conditions is important for accurate dose rate calculations for a specific CISF. Section III of this paper presents a series of sensitivity calculations that evaluated the effects on dose rate of the (1) air volume included in the simulations, (2) air density, (3) air relative humidity (RH), and (4) soil composition. Section IV describes SCALE 6.2.3 dose rate calculations for a proposed CISF,[7] and Section V presents conclusions.

II. SCALE 6.2.3 CAPABILITIES FOR RADIATION SOURCE TERM AND SHIELDING CALCULATIONS

Depletion and shielding calculation capabilities available in the SCALE 6.2.3 code system used to perform SNF radiation source term and dose rate calculations are described in this section.

II.A. Radiation Source Term Calculation Method

Assembly-specific radiation source terms for use in dose rate calculations were generated with ORIGEN Assembly Isotopics (ORIGAMI), a SCALE module dedicated to calculating nuclide inventories, decay heat, and radiation source terms for SNF assemblies based on axial burnup profile and/or variable pin power specifications. This code performs fast Oak Ridge Isotope Generation and Depletion (ORIGEN)[8] calculations using pre-generated ORIGEN cross section

libraries. The radiation source terms included photon and neutron sources in the fuel region and the ^{60}Co activation sources in fuel assembly hardware regions and nonfuel hardware. The characteristics of the design basis fuel assembly (i.e., fuel assembly type, initial enrichment, average burnup, and decay time) and nonfuel hardware were obtained from final safety analysis reports (FSARs) prepared by cask vendors for the cask systems that would be used at the modeled CISF. These radiation source terms, saved in the ORIGEN ft71 binary file, were directly used in MAVRIC source specifications.

II.A.1. ORIGEN Validations

The ORIGEN sequence computes isotopic compositions in SNF for over 1,000 nuclides. ORIGEN has been validated extensively for a wide range of applications, including reactor analysis, SNF dry storage and transportation, and fuel reprocessing.[8] This sequence was evaluated against approximately 200 fuel assembly decay heat measurements for various pressurized water reactor (PWR) and boiling water reactor (BWR) commercial SNF assemblies with burnups of up to 51 GWd/MTU for PWRs and 47 GWd/MTU for BWRs and cooling times ranging from ~ 2.5 to 27 years after fuel discharge from the reactor to ensure satisfactory performance. The neutron and gamma radiation sources and energy spectra generated by ORIGEN were also compared with measurements for individual radionuclides for validation.

II.B. Shielding Calculation Method

Dose rate calculations were performed with the MAVRIC shielding analysis sequence in SCALE, which employs state-of-the-art hybrid variance reduction capabilities[9,10] developed at ORNL to generate high-fidelity dose results. MAVRIC features (1) multigroup and continuous-

energy Monte Carlo transport capabilities, (2) automated variance reduction, (3) point detector, region, and mesh tallies, (4) simplified source term descriptions (e.g., direct use of radiation source terms from ORIGEN ft71 binary files), and (5) automated post-processing of mesh tally files.

Variance reduction refers to methods and techniques that significantly increase the efficiency of Monte Carlo radiation transport calculations. The variance reduction method referred to as *forward-weighted consistent adjoint driven importance sampling* (FW-CADIS)[10] is used to obtain dose rate estimates with good statistical accuracy everywhere outside a heavily shielded system. This method performs both forward and adjoint discrete ordinates calculations with the Denovo discrete ordinates code[11] to generate space- and energy-dependent scalar forward and adjoint fluxes. These fluxes are subsequently used by MAVRIC to generate energy- and space-dependent source biasing and particle importance parameters (weight windows). The adjoint calculation solution identifies the spatial regions and energy ranges of the radiation source that make important contributions to dose rate within a geometry region of interest. The forward solution is used to optimize dose rate estimation.

II.B.1. MAVRIC Validations

The MAVRIC shielding code has been validated by comparing its results with experimental measurements that tested photon and neutron transmission through various shielding materials.[4] An additional MAVRIC validation calculation is provided in this paper. The unshielded source configuration of the well-known Kansas State University (KSU) photon skyshine benchmark experiment[12,13] was simulated with MAVRIC. This experiment has been analyzed with MCNP and included in Shielding Integral Benchmark Archive & Database (SINBAD),[14] available from the Radiation Safety Information Computational Center (RSICC) at ORNL. In this experiment,

exposure rates due to skyshine radiation produced by three different ^{60}Co sources of 10.33 Ci, 229.1 Ci, and 3,804 Ci were measured in air at distances of 50, 100, 200, 300, 400, 500, 600, and 700 m from the source. Each ^{60}Co photon source was placed within a 228.6 cm (7.5 ft) high annular concrete silo with 91.44 cm (3 ft) thick walls. Concrete wedges and lead bricks were installed on the top of the silo to define a 150.5° vertical-conical beam. Each source was horizontally centered within the silo and raised 2.54 cm above the top of one of the two special purpose-built transportation casks residing inside the silo. The elevation of the source was 1.98 m above the grade. A 25.4 cm diameter, argon-filled, high-pressure ionization chamber (HPIC) was used to measure the 4π-skyshine gamma radiation exposure rate at 1 m above grade. The measured exposure rates were reported per source activity unit. The ^{60}Co sources consisted of nickel-plated ^{60}Co pellets, and the spectra of the gamma rays exiting the three ^{60}Co sources were determined by Monte Carlo simulations of radiation attenuation within source materials.[15] The benchmark exposure rate measurements were performed on Sept 26, 1977. The estimated air density for that day was 1.096 kg/m^3, which was based on reported environmental conditions that day including a temperature of 304K, local pressure of 962 mb (96.2 kPa), and relative humidity of 32.8%.[15]

Only the measurements at 50, 100, 200, 400, 600, and 700 m were included in the SINBAD database.[14] A total measurement uncertainty of approximately 7% has been estimated,[12] which includes the uncertainties associated with a required HPIC energy response correction and the reported ^{60}Co source strengths. The uncertainty associated with the benchmark MCNP model[14] was approximately 8%. The largest model uncertainty was attributed to the modeled air density and composition.

The response functions in the MAVRIC calculations were the ICRU-57 conversion coefficients[16] from photon air kinetic energy release in materials (kerma) in units of

(Gy/h)/(photon/cm^2/s). The effect of model uncertainty was not evaluated in this paper. It is assumed to be similar to the 8% value determined based on MCNP benchmark evaluations. A comparison with the benchmark experimental data is shown in Table I. The agreement between MAVRIC and benchmark experimental data is within measurement 2σ uncertainty.

III. SENSITIVITY CALCULATIONS

A series of sensitivity calculations were performed to determine the effects on dose rate of various model parameters simulating local environment and atmospheric conditions. The surrounding air and soil have significant scattering effects on radiation, phenomena known as *skyshine* and *groundshine*, respectively. Therefore, the dose rate at each location outside a storage facility is the total of the dose rate produced by the direct radiation, the dose rate produced by the radiation scattered in air (i.e., skyshine), and the dose rate produced by radiation that reemerges into the air as a result of scattering within the ground (i.e., groundshine). Although surrounding air has a very low mass density compared with other materials, the ample volume of air included in a skyshine calculation model has significant attenuation and scattering effects on radiation. For an SNF storage cask, the skyshine contribution to total dose rate has been shown to increase with increasing distance from the cask for both photon and neutron dose rates.[6]

All sensitivity calculations presented in this section used a single vertical SNF storage cask, [17] the model of which is illustrated in Fig. 1. This cask model describes a canister loaded with 24 PWR SNF assemblies of identical initial enrichment (3.59 wt% ^{235}U), average burnup (43 GWd/MTU), and decay time (5 years). The fuel assembly materials were homogenized within the active fuel region, lower end assembly hardware, gas plenum region, and upper end assembly

hardware. The earth-air interface was represented as a flat surface because the skyshine calculation models typically neglect local topographic features. The soil was modeled to a depth of 1 m. The base model has a cylindrical boundary with a radius of 1,300 m and a height of 1,301 m. Data on US standard atmosphere[18] as well as other data that were made available by various weather stations were used in this paper to determine the air density and composition at various elevations and atmospheric conditions. The US standard atmosphere is an inert gas (i.e., dry air), static atmospheric model describing average air temperature, pressure, and density as a function of altitude. Air density primarily depends on the standard variation of air pressure with altitude and the influence of temperature variations with height on the air pressure. It should be noted that weather reports provide air pressure adjusted to sea level, not the actual atmospheric pressure at the weather station location. Therefore, the reported air pressure in weather records must be uncorrected to obtain the atmospheric pressure at the weather station location.

Dose rates were calculated above the ground at selected distances up to 1,000 m from the vertical axis of the cask. The dose rate tally regions were modeled as concentric 1 m wide and 2 m high annuli above the ground. The dose rate values were calculated with a maximum relative error of approximately 4%. All graphs presented in this section show the dose rate estimate ± 3 sigma statistical uncertainty. Secondary gamma radiation from neutron interactions with matter is included in the photon dose rate.

The following model parameters were analyzed in the sensitivity study.

- Air volume
- Air density

- Multilayers of air with varying density as a function of height versus uniform volumetric air density
- Air relative humidity
- Soil water content

III.A. Air Volume

Ample volumes of air and soil extending beyond the location of interest for dose rate calculation are typically included in the calculation model to properly simulate important radiation scattering events that contribute to the dose rate at that location. The required volume of air is problem dependent. To determine the volume of air required to accurately determine dose rate at a location of interest, the volume of air beyond that location was gradually increased until minimal effects were noticed on the total dose rate at that location.

The radial and axial extents of the air volume required to accurately evaluate the dose rate at a distance of 1,000 m from the cask were evaluated separately. Dry air with a mass density of 1.114 kg/m^3 was used in the calculations. Three different models with different radial extents, 1,000 m, 1,100 m, and 1,200 m, were used for the radial extent study. The column of air was 1,300 m high above the ground in all these models. The dose rates produced by these models were compared with the dose rate produced by a model that included 1,300 m of air in the radial direction. The ratio of dose rate obtained for each of the three models to the dose rate obtained with the model including 1,300 m of air in the radial direction is presented in Fig. 2 as a function of distance from the cask. These simulations show that the model would need to include at least 100 m of air in the radial direction beyond the dose rate location of interest to accurately evaluate

neutron and photon dose rates at that location. The impact of not modeling enough air beyond the radial location of the dose rate of interest is higher for neutrons than for photons because neutron scattering, in general, approaches an isotropic angular distribution for most nuclides and photons, on average, are scattered in the forward direction.

The effects of the height of the air column used in the model were analyzed with respect to skyshine neutron and photon dose rates. The model included the cask model shown in Fig. 1 and a berm surrounding the cask. The berm was modeled as a cylindrical shell made of soil and located 30 m from the cask. The height and the thickness of the cylindrical shell were 6 m and approximately 2.5 m, respectively. The height of the air column above the ground was incrementally increased from 100 m to 700 m while maintaining an air radial extent of 1,300 m from the cask.

The effects of the height of the air column on shyshine dose rates above the ground are illustrated in Fig. 3 as a function of the distance from the cask vertical axis. The values shown in the graphs represent (a) the ratio of the skyshine neutron dose rate produced by a height of the air column varying from 100 m to 700 m to the dose rate based on a 700-m high column of air and (b) the ratio of the skyshine photon dose rate produced by a height of the air column varying from 100 m to 500 m to the dose rate based on a 500-m high column of air. The statistical errors were less than 4% for neutron dose rate and less than 2% for the photon dose rate. These statistical errors are not shown in the graph to provide a clear view of the trends. The parametric calculations show that the required minimum heights of the air column above the ground would be 600 m and 400 m to accurately estimate the skyshine neutron dose rate and photon dose rate, respectively, up to 1,000 m from the cask.

In the case of the vertical SNF cask used in this study, the photon dose rate dominates the total dose rate. The neutron skyshine component is approximately 80% of the total neutron dose rate at dose rate locations beyond 400 m from the cask. This contribution is approximately 35% for the skyshine photon dose rate at locations beyond 400 m from the cask.

III.B. Air Density Effects

Dose rate above the ground as a function of distance from the cask vertical axis was calculated using dry air at two different air densities: (1) 1.225 kg/m^3, i.e., the standard air density at sea level, and (2) 1.114 kg/m^3, i.e., a 9% air density decrease, which is the average standard air density from 950 m to 1,000 m above sea level. Uniform air density within the boundary of the model was used in these calculations. The geometry model included a column of air that extended 1,300 m in the radial direction and 1,300 m in the axial direction. The ratio of dose rate based on standard dry air with a density of 1.114 kg/m^3 to dose rate based on standard dry air with a density of 1.225 kg/m^3 is shown in Fig. 4 as a function of distance from the cask vertical axis. Both photon and neutron dose rates increased with decreasing air density, and the relative increase is directly proportional to the distance from the cask. For this example, the total/photon/neutron dose rate increase was approximately 60% at 1,000 m from cask.

III.C. Air Composition Effects

Air at various locations and atmospheric conditions may have the same mass density. The effects on neutron and photon dose rates of four different conditions yielding the same air density (1.114 kg/m^3) were analyzed in this paper. The four cases included dry air and moist air with three different sets of temperature, relative humidity, and barometric pressure. The humid air parameters were (1) 310.93 K (100 °F), 100% RH, and 101.83 kPa (30.07 inHg); (2) 299.82 K (80 °F), 50%

RH, and 98.71 kPa (29.15 inHg); and (3) 297.04 (75 °F), 30% RH, and 97.53 kPa (28.80 inHg). The far-field dose rate calculations showed that air composition at constant mass density is only important for the neutron dose rate. As expected, dry air produces higher neutron dose rates than moist air with same mass density. The ratio between neutron dose rate in dry air to dose rate in humid air is presented in Fig. 5 as a function of distance from the cask for the three different humid air cases. The gamma dose rate was not sensitive to dry and humid air that had same mass density.

III.D. Altitude Effects

Air density decreases with increasing altitude, as indicated in the U.S. Standard Atmosphere 1976 standard.[18] For example, the air density of the standard atmosphere decreases from 1.225 kg/m^3 at sea level to 1.1673 kg/m^3 at an altitude of 500 m. Therefore, a multilayer model with decreasing air density from bottom to top would better represent the actual air density variation than a single layer of air with uniform density.

Dose rates were calculated above the ground as a function of distance from the cask using multilayer and single-layer models. In the multilayer air model, the air was subdivided into 50 m thick horizontal layers. The mass density values for these air layers were obtained from the US standard atmosphere data.[18] The single-layer air model used a uniform air density, which was also used in the air layer located above the ground in the multilayer model. The difference in dose rate values produced by the two different air models was within statistical uncertainty for both neutrons and photons at the analyzed locations up to 1,000 m above the ground. This outcome may be the result of (1) the direct radiation being a significant contributor to the total dose rate and (2) the multilayer model producing both increasing effects (e.g., less attenuation in the upper air layers)

and decreasing effects (e.g., less backscattering events in the upper air layers) on the dose rate above the ground.

The average density of the air over a certain height above the ground may be used to capture the altitude effects on air density in the single-layer air model. This average air density is lower than the air density above the ground because the air density decreases with increasing altitude. Using dry air with the average density in the single-layer air model would produce conservative neutron and photon dose rates above the ground based on the results of the sensitivity analysis presented in Section III.B. Calculations were performed using the average standard air density from 950 m to 1650 m above sea level of 1.079 kg/m^3. The increases in the neutron, photon, and total dose rates at 1,000 m from the cask were 20%, 16%, and 16%, respectively, compared with the values based on the 1.114 kg/m^3 air density.

III.E. Air Temperature and Relative Humidity Effects

Humid air weighs less than dry air at the same temperature because a fraction of dry air is replaced by water and the molecular weight of moist air is lower than that of dry air. For example, the molecular weight of moist air would be 27.50 g/mole for moist air consisting of 90% dry air and 10% H_2O compared with ~28.56 g/mole for dry air. Air humidity varies widely in the troposphere, depending on its proximity to sources and sinks of moisture. Observational data show a variation in the vapor content of air from 0.1 to 35,000 ppm at sea level.[18] However the record high values decrease with increasing altitude because the amount of water vapor that air can contain decreases exponentially with falling temperature.[18] The effects of air temperature and humidity on dose rate were analyzed in this study relative to dry air corresponding to standard atmosphere[18] (1) at sea level and (2) at a higher altitude of 970 m. The standard air at sea level has

a pressure of 101.325 kPa (~30 inHg), a temperature of 288.17 K, and a mass density of 1.225 kg/m^3. These parameters for standard air at the higher elevation analyzed were 90.42 kPa (~26.7 inHg), 281.98K, and 1.114 kg/m^3.

One set of calculations used an air temperature of 310.928 K (100 °F) and a relative humidity of 100%, which were among record high temperature and humidity values at the analyzed high elevation. Under these conditions, the mass density values for the moist air were 1.112 kg/m^3 at sea level and 0.989 kg/m^3 at the higher elevation (i.e., approximately 10% decrease from the standard dry air mass density). The effects on dose rate of these record high conditions relative to the standard dry air described in the paragraph above are illustrated in Fig. 6 (a) for sea level and (b) for the higher elevation. These graphs show that the record high temperature and humidity had very similar effects on photon and neutron dose rates relative to standard dry air at each of the elevations analyzed. The photon dose rate is higher in moist air relative to dry air because moist air has a lower mass density, which decreases the rate of attenuation. The relative difference between photon dose rate in the moist air and the dose rate in the standard dry air steadily increased with increasing distance from the cask up to ~70% at 1,000 m from the cask vertical axis. The neutron dose rate however is lower in moist air, which contains hydrogen, than in dry air. The net effect on total dose rate depends on the relative contributions of the photon and neutron dose rates to the total dose rate. The far-field dose rate for the analyzed cask is dominated by the gamma radiation, as shown in Fig. 6, and the total dose rate exhibited an increasing trend with increasing distance from the cask, similar to that of the photon dose rate.

The effects of average atmospheric conditions on dose rate were also analyzed relative to standard dry air at the higher elevation. The average air temperature, pressure, and RH for the higher elevation were 291.483 K (65 °F), 90.52 kPa (26.73 inHg), and 56%, respectively, which

produce an air density of 1.076 kg/m^3. The relative effects of average atmospheric conditions on photon and neutron dose rates, presented in Fig. 7, are significantly lower than the relative effects of record high temperature and relative humidity conditions. The photon dose rate assuming average temperature and humidity values only increased by 20% at 1,000 m from the cask, compared with an ~70% increase at this location for record high temperature and humidity.

III.F. Groundshine Effects

The dose rate in the air regions above the ground includes contributions from the direct radiation and the groundshine. An infinite air medium approximation without taking into account groundshine would underestimate dose rate in the regions above the ground. Groundshine contribution to dose rate above the ground was evaluated using a geometry model that included a layer of soil 1 meter in depth and another model in which the soil was replaced with air. The ratio between the dose rate values produced by these two models above the ground represents an estimate of the groundshine contribution to dose rate. Soil composition is expected to affect the groundshine dose component because of different scattering and neutron-slowing-down properties of the various soil components. The concentration of hydrogen in soil is important because neutron interaction with hydrogen nuclei effectively reduces the neutron energy to very low values. Water content in soil depends on water availability and soil porosity, which varies from approximately 40% for sandy soils to 52–64% for loamy soils.[19] Pavement materials such as concrete or asphalt also contain hydrogen. Secondary gamma rays are also generated as a result of neutron slowing down and capture in the soil/pavement material. The sensitivity analysis in this paper evaluated the groundshine effects of two different soil compositions: the average US earth composition[20] without water content and a soil composition containing 2.1% hydrogen by weight.

The ratio between dose rate produced by a model specifying either dry or wet soil to the dose rate produced by a model that uses air in place of soil is shown in Fig. 8 as a function of distance from the cask. The groundshine contribution to the total neutron dose rate above the ground strongly depends on the water content in soil. Neutron dose rate increases due to groundshine effects were approximately 75% and 180% for wet soil and for dry soil, respectively, at locations beyond 400 m from the cask. The groundshine contribution to the gamma dose rate above the ground was approximately 20% for both soil compositions analyzed.

The energy spectrum of groundshine radiation is also important because harmful biological effects increase with higher dose rates. The effects of the scattering medium on the neutron energy spectrum are illustrated in Fig. 9. Compared with dry soil or air medium, wet soil has moderating effects on neutrons from neutron interactions with the hydrogen nuclei, as illustrated by the low energy region of the neutron spectra. This analysis shows that modeling dry soil is conservative with respect to neutron dose rate above the ground. However, for radiation sources dominated by gamma radiation, the effects on dose rate of water content in the soil would be insignificant.

IV. CISF DOSE RATE CALCULATIONS

To illustrate SCALE's capability to simulate dose rates produced by a large CISF, dose rate calculations were performed for a proposed CISF in Andrews County, Texas.[7,21] The Interim Storage Partners (ISP) Phase 1 CISF would store 5,000 metric tons of heavy metal (MTHM) SNF and up to 231.3 MT of GTCC waste in Nuclear Assurance Corporation (NAC) vertical concrete casks (VCCs) and NUHOMS® horizontal storage modules (HSMs). Six different storage systems would be used to store SNF assemblies and GTCC waste, including the NAC-Universal Multi-

Purpose Storage (UMS) System,[22,23] NAC-Multi-Purpose Canister (MPC) Storage System,[24,17] MAGNASTOR Storage System,[25,26] NUHOMS®-MP187 Storage System,[27,28] Advanced Standardized NUHOMS® Storage System,[29,30] and the Standardized NUHOMS® 61BT/61BTH Type 1 Storage System.[31] The design basis fuel assemblies of these storage systems define bounding photon and neutron radiation sources for a wide range of PWR and BWR fuel types, average assembly burnup, and cooling times (e.g., from a 25 GWd/MTU average assembly burnup value and a 2.3-year cooling time to a 62 GWd/MTU average assembly burnup value and a 21.4-year cooling time).

IV.A. CISF Model

The analyzed storage pad configuration consisted of 467 (319 vertical and 148 horizontal) storage casks. The purpose of the calculations was to compute dose rates above the ground as a function of distance from the facility and determine the location of the 25 mrem/yr dose rate contour. The CISF model included the storage pad, surrounding air, and soil. A three-dimensional view of the Phase 1 storage pad model is shown in Fig. 10. The thickness of the concrete pad was 30 cm, and the soil was modeled at a depth of 1 m to account for radiation scattering and absorption in soil. The size of the geometry model was approximately $4.2 \times 4.1 \times 2.0$ km^3. Local atmospheric conditions were simulated using US standard atmosphere data that provide dry air temperature, pressure, and density as a function of altitude for a standard atmosphere model. The air column in the geometry model was subdivided into 40 vertical layers, each layer being 50 m high. A dry soil composition was used in the models.

Basic input data and assumptions used in cask vendor's safety analyses (e.g., cask design parameters and design basis assembly characteristics) were used to model each cask type and its

contents. The model templates and methods available in the Used Nuclear Fuel Storage, Transportation & Disposal Analysis Resource and Data System[32] (UNF-ST&DARDS) were instrumental in the CISF calculation. The UNF-ST&DARDS, which is developed at ORNL, includes the capability to perform dose rate calculations for SNF transportation packages based on the actual physical and nuclear characteristics (i.e., assembly design, burnup, initial enrichment, and post-irradiation cooling time) of the as-loaded SNF.[33] The degree of geometry detail in the cask models is illustrated in Fig. 11. The design basis fuel assembly was typically modeled as four axial regions: the upper end fitting region, upper gas plenum region, active fuel region, and lower end fitting region. Each axial region was represented as homogenous material within its geometry boundary with a mass density and elemental compositions derived from assembly hardware materials and weights.

IV.B. MAVRIC Parameters

The FW-CADIS method was used to generate a space- and energy-dependent importance map and consistent biased source distributions. The MAVRIC sequence in SCALE 6.2.3 does not have parallel computing capabilities, and its overall efficiency depends on the input specifications for mesh grid geometry and discrete ordinates parameters for the discrete ordinates calculations used to generate variance reduction parameters for Monte Carlo simulations. For the FW-CADIS method in MAVRIC, the user supplies a mesh for the coarse-mesh forward and adjoint deterministic calculations that are used to create the importance map and consistent biased source distribution. The mesh, while coarse compared with a production-level discrete ordinates

calculation, still needs enough refinement to capture the major material changes and divide the source region for biasing. A mesh that captures all the details of the vast number of sources present in a CISF model would require more memory than current computers have. Therefore, the dose contribution from each cask to the site dose was determined in a MAVRIC calculation using the complete site geometry (all loaded casks present) but with radiation sources only specified for the analyzed cask. A total of 467 independent calculations were performed to obtain the dose rate maps produced by each storage cask. The 467 individual dose rate maps were added together to obtain the total site dose rate map up to 2 km from Phase 1 CISF. A single processor was used for each case. The maximum computer time for each Monte Carlo simulation was 2 days to ensure a maximum statistical relative error < 20% for the highest dose produced by each storage cask along the estimated controlled area boundary.

The adjoint source was specified within a volume of air outside the storage pad and extending from the top of the soil to 2 m above the soil. This is the geometry region of the model in which the dose rate is expected to be calculated with significant accuracy because variance reduction parameters were optimized for the dose rate in that region. Dose rates were calculated within a geometry mesh with a voxel size of 15.24 m × 15.24 m × 2 m. The mesh tally only had one cell in the vertical direction, which extended from the top of the soil to 2 m above the soil. The ANSI/ANS 6.1.1-1977 neutron and photon flux-to-dose-rate conversion factors[34] were applied to the flux estimates to obtain dose rates.

For the importance map and source biasing calculations, a cask-specific Denovo mesh grid with finer mesh was used for the volume of the analyzed storage cask and its adjacent casks, but a coarse mesh was used elsewhere. A fine geometry mesh enables adequate representations of materials and radiation sources in the most important regions of the problem (i.e., the analyzed

cask). Equally important is the use of a coarse Denovo mesh in the geometry regions where radiation interactions with matter are rare events so that the computer time dedicated to those events is optimized. The starting source for one of the vertical casks is illustrated in Fig. 12. The figure shows a fine mesh within the analyzed cask and within the concrete wall of the adjacent casks, which scatters particles into the sky.

IV.C. Dose Rate Map

The annual dose map for the Phase 1 CISF and the surrounding air is presented in Fig. 13. This annual dose map was obtained by summing the uncorrelated space-dependent dose rate values of the mesh tallies from the 467 separate calculations. The relative statistical errors associated with dose values are less than 5%, 10%, and 20% for most of the mesh up to a distance of 1 km, 1.7 km, and 2 km from the pad, respectively. Based on the calculations described in this paper, the minimum distance from the Phase 1 storage pad to the 25 mrem/yr contour is 623 m (0.387 miles) in the N-NE direction, 594 m (0.369 miles) in the S-SW direction, and 533 m (0.331 miles) in the E-SE direction and the W-NW direction. At locations with an approximate annual dose of 25 mrem, the relative statistical error was approximately 1%.

V. CONCLUSIONS

This paper presents the radiation source term and shielding calculation capabilities of the SCALE 6.2.3 code system developed at ORNL and demonstrates SCALE's capability to simulate far-field CISF radiation dose rates. The Phase 1 storage pad of the CISF, proposed to be constructed and operated in Andrews County, Texas, was modeled, and the dose rate was computed above the ground at locations up to 2 km from the pad using SCALE 6.2.3. The method

presented in this paper uses a detailed Monte Carlo radiation transport simulation in one step from source to dose rate. A series of independent simulations was made using the complete site geometry (all casks present) but with only one cask containing its source to obtain the dose rate maps produced by each storage cask. The CISF dose rate map was obtained by adding the dose rate maps produced by the independent individual cask simulations, and the 2-D dose rate contour of the annual dose rate of 25 mrem was determined at approximately 600 m from the center of the evaluated storage pad. Ample volumes of air and soil extending beyond the location of interest for dose rate calculation were included in the Phase 1 CISF model to properly simulate important radiation attenuation and scattering events that affect far-field dose rates. Although the surrounding air has a very low mass density compared with other materials, the ample volume of air included in a skyshine calculation model has significant attenuation and scattering effects on radiation. A series of sensitivity calculations are presented to illustrate the importance of selecting appropriate air volume, mass density, and composition for site-specific CISF dose rate calculations. Dry soil and soil containing water were also analyzed to determine their effects on groundshine radiation, which is an important component of the far-field dose rate above the ground. All sensitivity analyses were performed using a single vertical concrete cask. The effects of various air and soil parameters on dose rate above the ground were evaluated as a function of distance up to 1,000 m from the cask center. The specific results of the sensitivity study presented in this paper are applicable to vertical concrete casks and the range of air/soil parameters analyzed in the paper and may not be applicable to other types of SNF storage casks (i.e., underground or horizontal storage casks) and air/soil parameters. However, the sensitivity studies in this paper show general sensitivities and trends of far-field dose rates to air density and water contents in air and soil.

Ample volumes of air and soil extending beyond the location of interest for dose rate calculation are typically included in the calculation model to properly simulate important radiation scattering events that contribute to the dose rate at that location and obtain unbiased dose rate estimates. The sensitivity calculations showed that skyshine neutron dose rate calculations require larger volumes of air to be included in the model than skyshine photon dose rate calculations. To accurately calculate the neutron dose rate above the ground at 1,000 m from the single cask, the minimum required width of the air volume in the model was 1,200 m (i.e., 200 m beyond the dose rate location) and the minimum required height of the air above the ground was 600 m. These requirements were 1,100 m for the air width and 400 m for the air height in the case of the photon dose rate for the same cask. If the model contained insufficient volume of air, dose rates would be underestimated by various degrees depending on the dose rate location and the height of the air volume modeled. For example, the neutron and photon dose rates above the ground at 1,000 m from the cask were underestimated by approximately 90% and 65%, respectively based on a model that only included air up to 100 m from the ground.

Air density is a very important parameter for far-field dose rate calculations because air density affects both direct and skyshine dose rates. Air density primarily depends on the standard variation of air pressure with altitude and the influence of temperature variations with height on the air pressure. Far-field photon and neutron dose rates may be increased by decreasing the density of the air in the model. The photon and neutron dose rates above the ground at 1,000 m from the analyzed cask increased by approximately 60% for a decrease of 9% in dry air density. The rate of increase was constant as a function of distance from the cask.

Air humidity varies widely in the troposphere, depending on its proximity to sources and sinks of moisture. The effects of air temperature and humidity on dose rate were analyzed relative to dry

air corresponding to standard atmosphere.[18] Humid air weighs less than dry air at the same temperature because a fraction of dry air is replaced by water and the molecular weight of moist air is lower than that of dry air. Therefore, humid air has different effects on photon dose rate compared to neutron dose rate. Humid air produces a higher photon dose rate because of lower photon attenuation and a lower neutron dose rate because of the water content compared with standard air at same altitude and air pressure. The effect of air humidity and temperature on total dose rate would depend on the relative contributions of photon and neutron dose rates to the total dose rate. Average or record high relative humidity and temperature values for local atmospheric conditions may be used to calculate conservative far-field dose rates if the photon dose rate dominates the total dose rate.

Air at various locations and atmospheric conditions may have the same mass density. Dose rates were evaluated for dry air and different air relative humidity and temperature conditions yielding the same air mass density. The far-field dose rate calculations showed that air composition at a constant mass density is only important for the neutron dose rate. Dry air produced higher neutron dose rates than moist air with the same mass density.

Air density decreases with increasing altitude, as indicated in the U.S. Standard Atmosphere 1976 standard.[18] The effects on dose rate of a single-layer air model versus a multilayer air model were evaluated. In the multilayer model, the air was subdivided into 50 m thick horizontal layers. The mass density values for these air layers were obtained from the US standard atmosphere data.[18] The single-layer model used a uniform air density, which was also used in the air layer located above the ground in the multilayer model. For the single cask analyzed in the sensitivity study, the dose rate values produced by the two different air models only differed within statistical uncertainties for both neutrons and photons at the analyzed locations up to 1,000 m above the

ground. The average density of the air over a certain air height (e.g., 700 m) above the ground may be used to conservatively capture the altitude effects on air density using a single-layer air model.

Sensitivity analyses showed that the groundshine neutron dose rate component, but not the groundshine photon component, is sensitive to the water content in the soil. Modeling dry soil would be conservative with respect to the neutron dose rate above the ground compared to modeling soil containing water. Compared with dry soil or infinite air medium, wet soil has moderating/absorption effects on neutrons from neutron interactions with the hydrogen nuclei. However, for radiation sources dominated by gamma radiation, soil composition effects would be insignificant.

The sensitivity studies provided in this paper emphasize the importance of conducting sensitivity studies on air volume and density and soil composition to developing an adequate model for far-field CISF dose rate calculations. For conservative far-field CISF dose rates, the air may be modeled using a mass density based on the altitude of the CISF location. Because the degree of conservatism would increase with decreasing dry air density, the average density of the air over a certain air height (e.g., 700 m) above the ground may be used in the model. Soil composition without water content may be used to produce higher neutron dose rates above the ground to satisfy conservative results.

ACKNOWLEDGMENTS

The work described in this paper was accomplished with funding provided by the US Nuclear Regulatory Commission and US DOE Office of Nuclear Energy.

VI. REFERENCES

1. US Code of Federal Regulations, "Licensing Requirements for Land Disposal of Radioactive Waste," Part 61, Title 10, "Energy."
2. US Code of Federal Regulations, "Licensing Requirements for the Independent Storage of Spent Nuclear Fuel, High Level Radioactive Waste, and Reactor-Related Greater than Class C Waste," Part 72, Title 10, "Energy."
3. *Spent Fuel Transportation Risk Assessment*, NUREG-2125, US Nuclear Regulatory Commission (2014).
4. D. E. PEPLOW, "Monte Carlo Shielding Analysis Capabilities with MAVRIC," *Nucl. Technol.*, **174,** *2*, 289 (2011).
5. B. T. REARDEN and M. A. JESSEE, Eds., "SCALE Code System," ORNL/TM-2005/39, Version 6.2, Oak Ridge National Laboratory (2016). Available from Radiation Safety Information Computational Center as CCC-834.
6. J. K. SHULTIS, "Radiation Analysis of a Spent Fuel Storage Cask," Report No. 290, Kansas State University (2000).
7. "License Application Docket 72-1050" (ML18206A483), Interim Storage Partners, LLC (2018).

8. I. C. GAULD et al., “Isotopic Depletion and Decay Methods and Analysis Capabilities in SCALE,” *Nucl. Technol.*, **174**, *2*, 169 (2011).

9. J. C. WAGNER and A. HAGHIGAT, “Automated Variance Reduction of Monte Carlo Shielding Calculations Using the Discrete Ordinates Adjoint Function,” *Nucl. Sci. and Eng.*, **128**, 186 (1998).

10. J. C. WAGNER, D. E. PEPLOW, and S. W. MOSHER, “FW-CADIS Method for Global and Regional Variance Reduction of Monte Carlo Radiation Transport Calculations,” *Nucl. Sci. Eng*. **176**, *1*, 37 (2014).

11. T. M. EVANS et al., “Denovo: A New Three-Dimensional Parallel Discrete Ordinates Code in SCALE,” *Nucl. Technol.*, **171**, *2*, 171 (2010).

12. M. L. ROSEBERRY, “Benchmark Skyshine Exposure Rates,” MS Thesis, Kansas State University (1977).

13. R. R. NASON et al., “A Benchmark Gamma-Ray Skyshine Experiment,” *Nucl. Sci. Eng.*, **79**, *4*, 404 (1981).

14. “Shielding Integral Benchmark Archive & Database,” SINBAD-2017.12, RSICC Data Library DLC-237.

15. R. H. OLSHER, H-H. HSU, and W. F. HARVEY, “Benchmarking the MCNP Monte Carlo Code with a Photon Skyshine Experiment,” *Nucl. Sci. and Eng*., **114**, *3*, 219–227 (1993).

16. International Commission on Radiation Units and Measurements, “Conversion Coefficients for Use in Radiological Protection Against External Radiation,” ICRU Report 57 (1998).

17. NAC International, “NAC Multipurpose Cask Final Safety Analysis Report,” Rev. 10, CoC 1025 Rev. 6, USNRC Docket Number 72-1025.

18. U.S. Standard Atmosphere 1976 – National Oceanic and Atmospheric Administration, US Government Printing Office, Washington, DC (1976).

19. M. KUTÍLEK and D. R. NIELSEN, *Soil: The Skin of the Planet Earth*, Springer Dordrecht, Heidelberg, New York, London (2015).

20. R. J. McCONN Jr. et al., “Compendium of Material Composition Data for Radiation Transport Modeling,” PNNL-15870 Rev 1, Pacific Northwest National Laboratory (2011).

21. “WCS Consolidated Interim Storage Facility Safety Analysis Report,” Rev. 2 (ML18221A408), Waste Control Specialists (2018).

22. NAC International, “Safety Analysis Report for the UMS® Universal Transport Cask,” Rev. 2, CoC 9270 Rev. 4, USNRC Docket Number 71-9270.

23. NAC International, “Final Safety Analysis Report for the UMS Universal Storage System,” Rev. 10, CoC 72-1015 Rev. 5, USNRC Docket Number 72-1015.

24. NAC International, “NAC-STC, NAC Storage Transport Cask Safety Analysis Report,” Rev. 17, CoC 9235 Rev. 13, USNRC Docket Number 71-9235.

25. NAC International, "MAGNASTOR® Final Safety Analysis Report," Rev. 6, CoC 1031 Rev. 4, USNRC Docket Number 72-1031.

26. NAC International, "Safety Analysis Report for the MAGNATRAN Transport Cask," Revs. 12A, 14A, and 15A, USNRC Docket Number 71-9356.

27. TN Americas, "NUHOMS®-MP187 Multi-Purpose Transportation Package Safety Analysis Report," NUH-05-151 Rev. 17, NRC Docket No. 71-9255.

28. TN Americas, "Rancho Seco Independent Spent Fuel Storage Installation, Final Safety Analysis Report," Volume I, ISFSI System, NRC Docket No. 72-11, Rev. 4.

29. TN Americas, "NUHOMS® -MP197 Transportation Package Safety Analysis Report," NRC Docket No. 71-9302, NUH09.101 Rev. 17.

30. TN Americas, "Updated Final Safety Analysis Report for the Standardized Advanced NUHOMS® Horizontal Modular Storage System for Irradiated Nuclear Fuel," NRC Docket No. 72-1029, ANUH-01.0150. Rev. 6.

31. TN Americas, "Updated Final Safety Analysis Report for the Standardized NUHOMS® Horizontal Modular Storage System for Irradiated Nuclear Fuel," NRC Docket No. 72-1004. NUH-003. Rev. 14.

32. R. A. LEFEBVRE et al., "Development of Streamlined Nuclear Safety Analysis Tool for Spent Nuclear Fuel Applications," *Nucl. Technol.*, **199**, *3*, 227 (2017).

33. G. RADULESCU et al., “Shielding Analysis Capability of UNF-ST&DARDS,” *Nucl. Technol.*, **199**, *3*, 276 (2017).

34. American National Standard Neutron and Gamma-Ray Flux-to-Dose-Rate Factors, ANSI/ANS 6.1.1-1977, American Nuclear Society, La Grange Park, Ill. (1977).

Table I

Comparison of Measured and Calculated Photon Skyshine Data

Distance from Source (m)	Source (Ci)	Exposure Rate (μR/h/Ci)		
		Measurement [a]	Calculation [b]	Difference [c] (%)
50	10.33	24.24 ± 3.41	25.54 ± 0.64	5.01
100	10.33	9.66 ± 1.35	9.79 ± 0.23	1.33
200	10.33	2.425 ± 0.340	2.561 ± 0.064	5.60
400	229.1	0.31 ± 0.04	0.345 ± 0.008	11.25
600	3804	0.0542 ± 0.0076	0.0559 ± 0.0013	3.11
700	3804	0.0244 ± 0.0034	0.0244 ± 0.0005	0.17

[a] Exposure rate $\pm 2\sigma$, where σ is equal to the benchmark measurement uncertainty of 7%.

[b] Exposure rate $\pm 2\sigma$, where σ is equal to the calculation statistical uncertainty.

[c] Percent difference between calculation and measurement values.

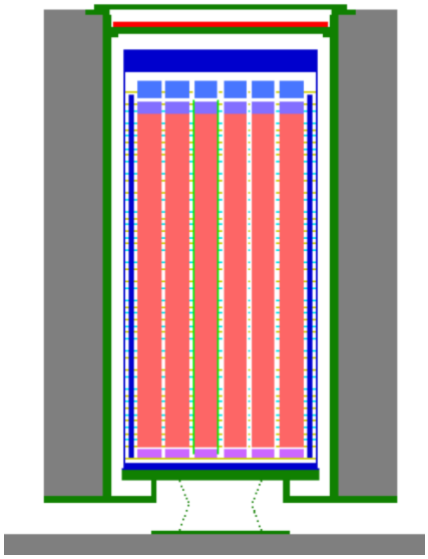

Fig. 1. Cross-sectional view of the SNF storage cask model used in sensitivity analyses.

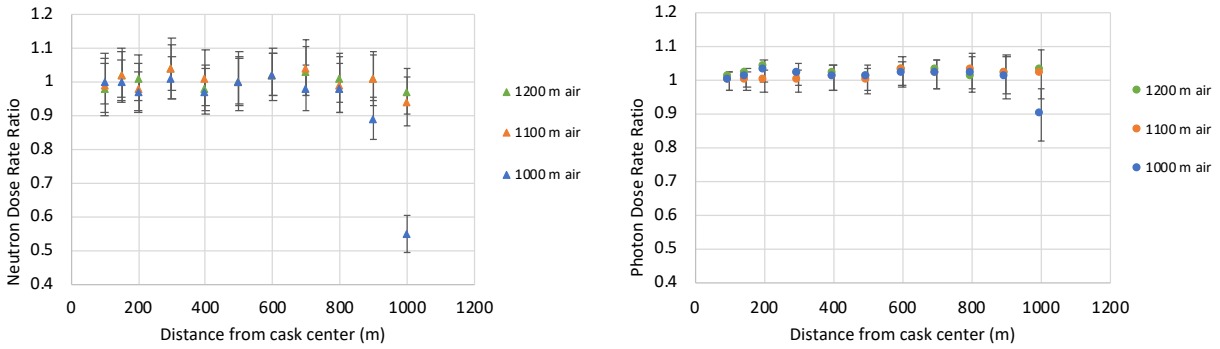

(a) (b)

Fig. 2. Ratio of dose rate based on the air radial extents of 1,000, 1,100, and 1,200 m to dose rate based on an air radial extent of 1,300 m from the cask vertical axis for (a) neutrons and (b) photons.

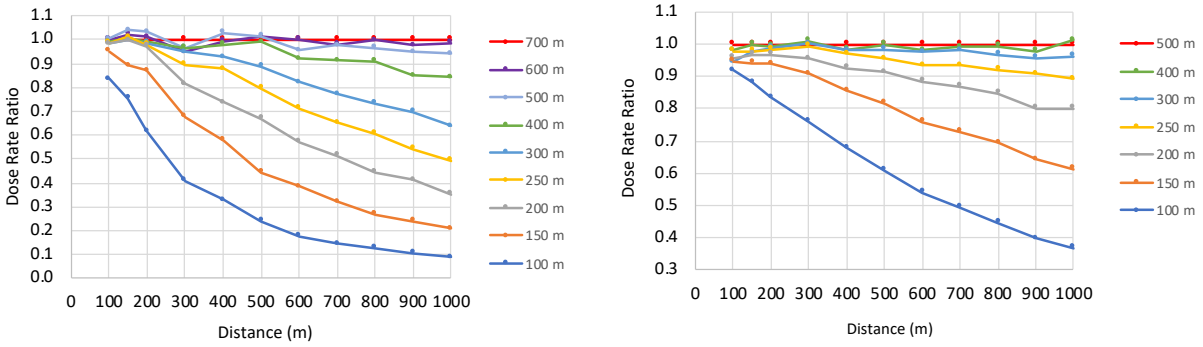

(a) (b)

Fig. 3. Effects of the height of the air column used in the calculation model on (a) shyshine neutron and (b) shyshine photon dose rates above the ground as a function of distance from the cask relative to (a) the skyshine neutron dose rate produced by a 700-m high column of air and (b) the skyshine photon dose rate produced by a 500-m high column of air.

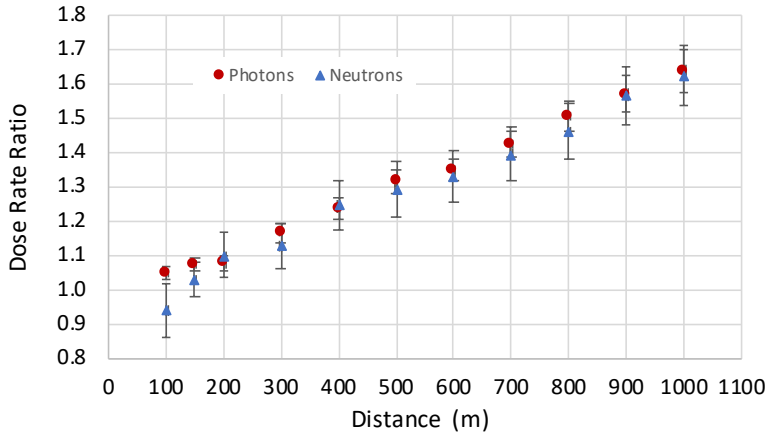

Fig. 4. Ratio of dose rate based on standard air with a density of 1.114 kg/m^3 to dose rate based on standard air with a density of 1.225 kg/m^3 as a function of distance from the cask.

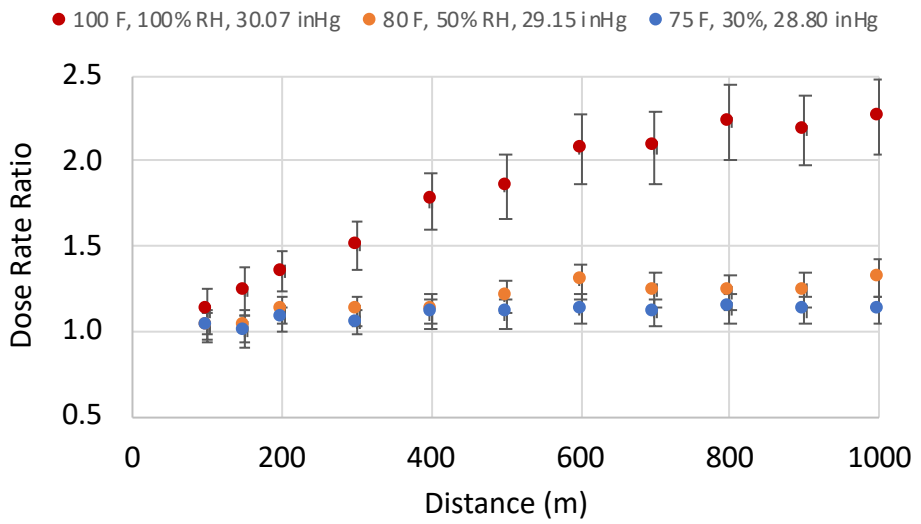

Fig. 5. Ratio of neutron dose rate in dry air to neutron dose rate in humid air at various temperature, humidity, and barometric pressure conditions assuming constant air mass density.

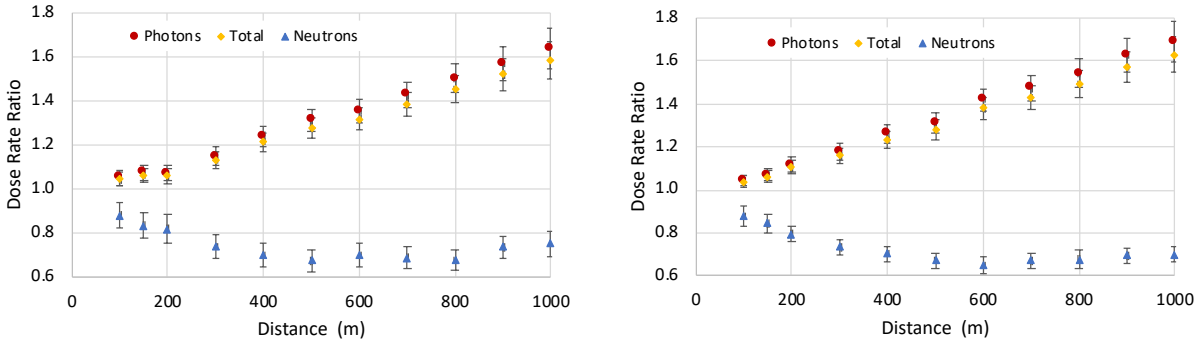

(a) (b)

Fig. 6. Effects on photon and neutron dose rates of record high temperature and RH relative to standard dry air at (a) sea level and (b) a 970 m elevation.

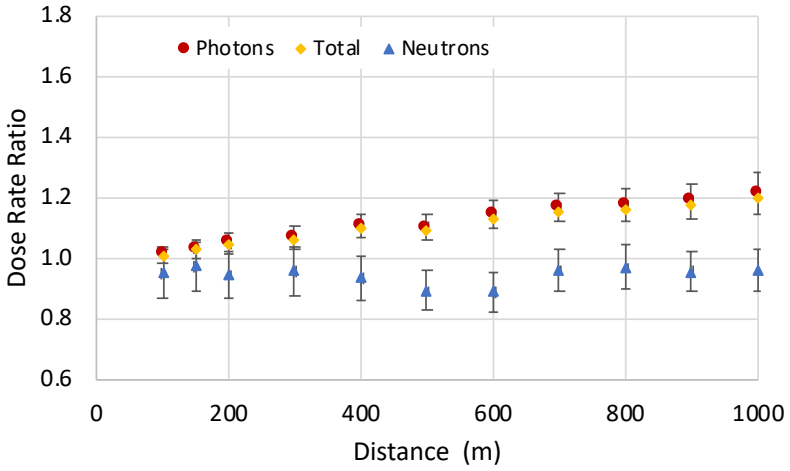

Fig. 7. Effects on photon and neutron dose rates of average temperature and relative humidity relative to standard dry air at a 970 m elevation.

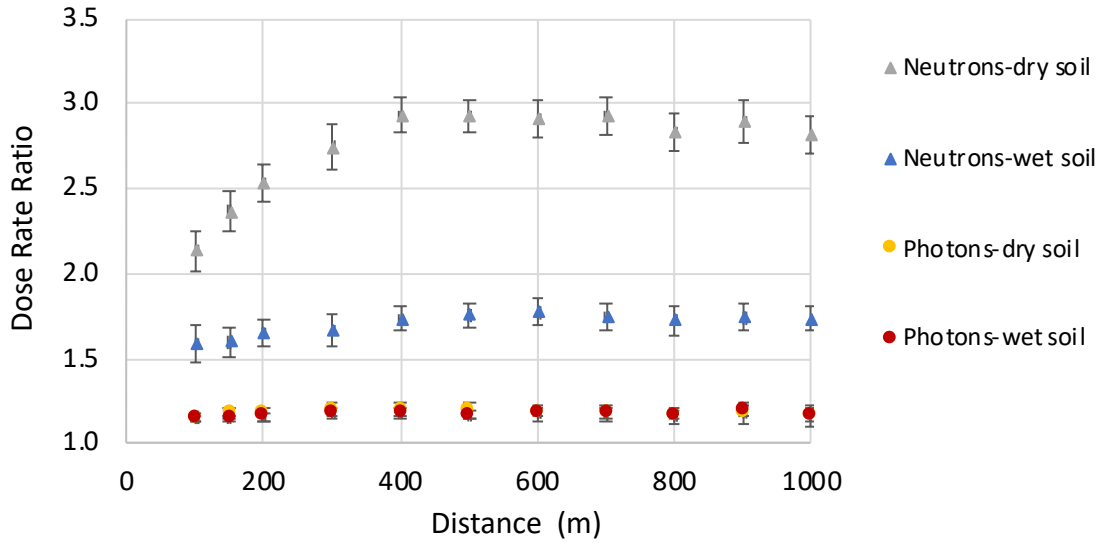

Fig. 8. Effects of dry soil and wet soil on dose rate above the ground relative to dose rate produced by a model that uses air in place of soil.

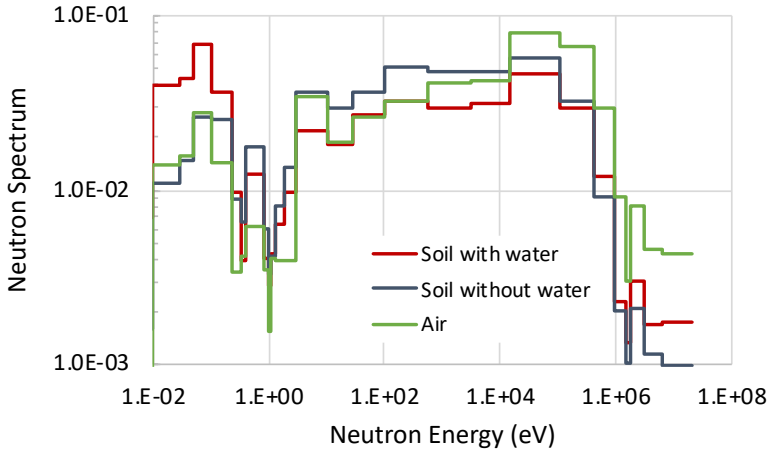

Fig. 9. Neutron energy spectra in air assuming different ground materials.

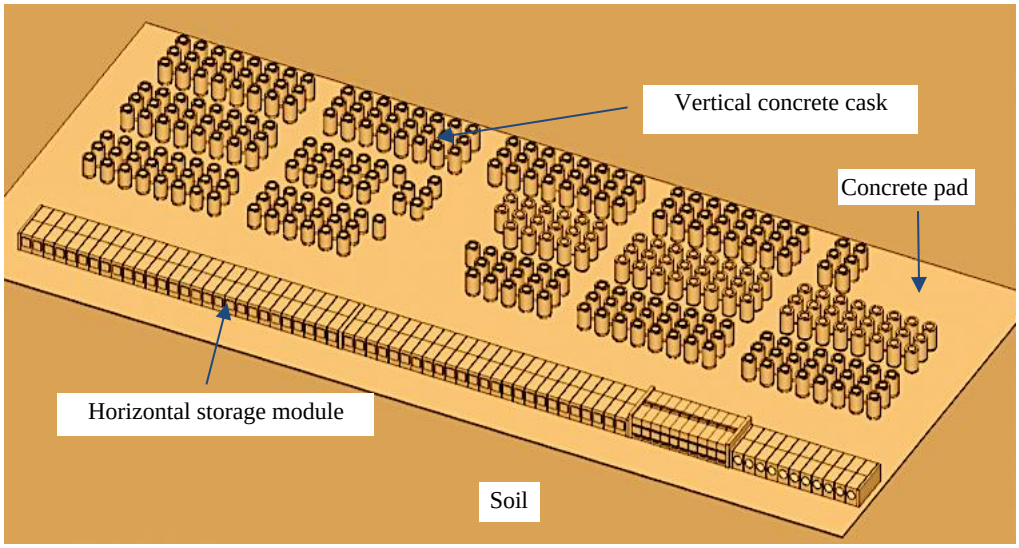

Fig. 10. Three-dimensional view of the CISF pad model.

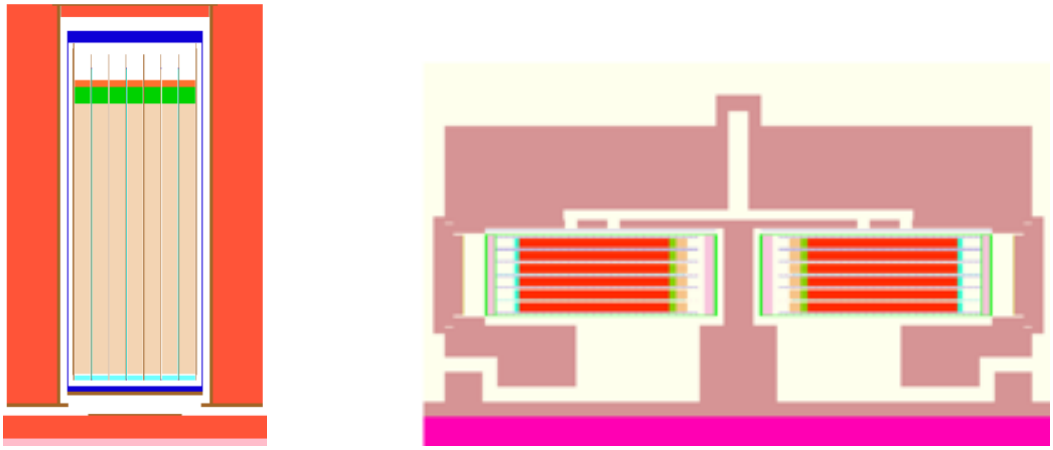

a b

Fig. 11. Vertical cross-sectional views of the models for a representative (a) vertical cask and (b) horizontal module.

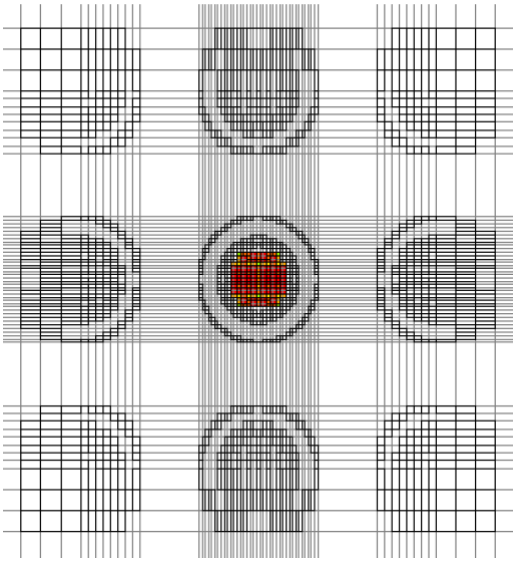

Fig. 12. Illustration of spatial discretization and starting source spatial distribution for a cask on the storage pad in Denovo calculations.

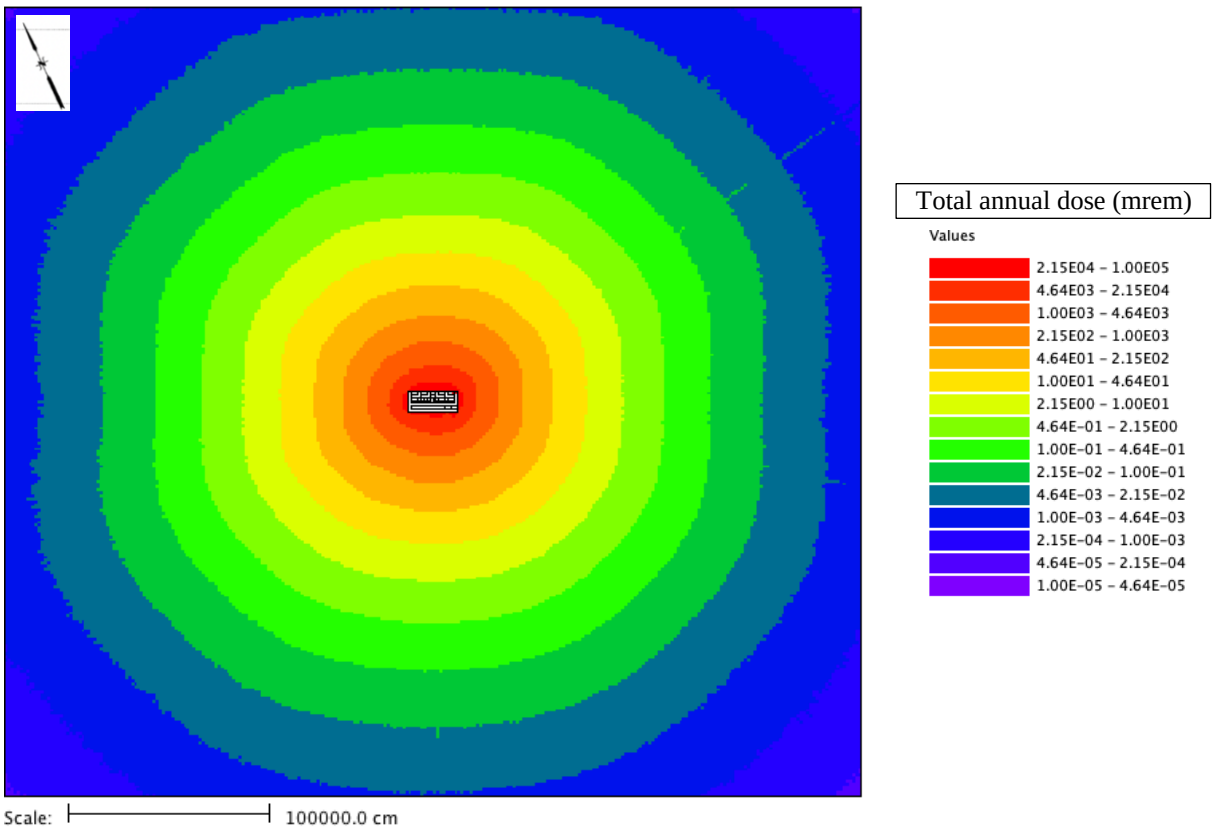

Fig. 13. Annual dose (mrem) for area surrounding the Phase 1 storage pad. Total area shown is 4.244×4.107 km^2.